JOBNAME: JPO 00#0 2011 PAGE: 1 SESS: 8 OUTPUT: Thu Mar 24 14:31:36 2011 Total No. of Pages: 14
/ams/jpo/0/jpo4504





# Tides in a System of Connected Estuaries

AMY F. WATERHOUSE AND ARNOLDO VALLE-LEVINSON

*Civil and Coastal Engineering Department, University of Florida, Gainesville, Florida*

CLINTON D. WINANT

*Scripps Institution of Oceanography, University of California, San Diego, La Jolla, California*

(Manuscript received 18 May 2010, in final form 4 October 2010)

ABSTRACT

The spatial structure of tidal amplitude and phase in a simplified system of connected estuaries, an idealized version of Florida's Intracoastal Waterway, is analyzed with a linear analytical model. This model includes friction, the earth's rotation, and variable bathymetry. It is driven at the connection with the ocean by a co-oscillating tide. Model results compare well with observations of pressure and currents in a section of the Intracoastal Waterway on the east coast of Florida. The comparison suggests that the waterway is highly frictional, causing the amplitude of the water elevation and tidal velocity to decrease away from the inlets to a minimum in the middle of the waterway. The local phase relationship between velocity and water elevation changed nonlinearly from 90° with no friction to 45° with maximum friction. In moderately to highly frictional basins, the phase lag was consistently less than 45°.

## 1. Introduction

As tides enter basins, a variety of interactions modify the tidal signal including friction, the earth's rotation, and bathymetry. Early works on co-oscillating tides found that observed tidal signals were superpositions of oppositely traveling Kelvin waves (Taylor 1921) and that energy was absorbed at the head of basins which accounted for the observed dissipation of tidal energy (Hendershott and Speranza 1971). As friction becomes important, the phase difference between velocity and elevation departs from the classical frictionless co-oscillating solution (Friedrichs and Aubrey 1994; Prandle 2003; Friedrichs 2010). Tidal propagation in shallow rivers was found to be more properly described as a diffusive process rather than a wave propagation phenomenon (LeBlond 1978; Friedrichs and Madsen 1992). Further studies on amplitude and phase changes in tidal channels with arbitrary lateral depth variations found that sea surface elevation was one dimensional along the estuary (Li and Valle-Levinson 1999). Velocities had strong lateral shear and were three dimensional, dependent on the lateral depth variations (Li and Valle-Levinson 1999).

Although the idealization of a semi-enclosed basin fits many realistic estuaries, there are also many systems of interconnected estuaries along coastlines. These systems can result from natural processes or they can be manmade, to facilitate navigation, as in the case of the Intracoastal Waterway on the east and Gulf coasts of the United States or the Dutch Wadden Sea in the Netherlands. These regions are often inhabited on both the mainland and barrier sides and are typically ecologically sensitive, very susceptible to anthropogenic activities. Flushing mechanisms and the subsequent health of these systems depend mostly on tidal and wind-driven circulation. Therefore, development and planning in these regions need rigorous evaluation of what physical mechanisms force the flow, including appropriate models.

An analytical model of tidal circulation in a semi-enclosed estuary (Winant 2007) is modified herein to represent the circulation in a system of two connected estuaries, as a building block for more complicated systems. The linear model assumes constant density and a no-slip bottom boundary condition and may include the effects of the earth's rotation. This model has been used to describe tidal flow in low to moderately frictional basins with one opening (Winant 2007) and residual flows in

*Corresponding author address:* Amy F. Waterhouse, Civil and Coastal Engineering Department, University of Florida, Gainesville, FL 32601.
E-mail: awaterhouse@ufl.edu

DOI: 10.1175/2010JPO4504.1

JOBNAME: JPO 00#0 2011 PAGE: 2 SESS: 8 OUTPUT: Thu Mar 24 14:31:36 2011 Total No. of Pages: 14
/ams/jpo/0/jpo4504





both tidally dominated (Winant 2008) and estuaries with gravitational circulation (Winant 2010). Dynamically important nondimensional parameters required for the model are $\alpha$, the horizontal aspect ratio of the basin (width to length); $\kappa$, the length of the basin to the wavelength of the tidal wave ratio; and $\delta$, the relative importance of friction to local accelerations. The parameters describing friction and relative length in this model are defined as

$$\delta = \sqrt{2K'/\omega' H'^2}, \quad \kappa = \omega' L'/\sqrt{gH'}, \tag{1}$$

where $K'$ is a constant vertical eddy viscosity, $\omega'$ is the frequency of the tide, $H'$ is the maximum basin depth, $L'$ is the length of the basin, $g$ is the gravitational acceleration, and $'$ represents a dimensional parameter. For our purposes, parameters $\delta$ and $\kappa$ are important, whereas rotation can largely be ignored. Previous studies have explained tidal flow with low friction conditions ($\delta \leq 1$; Winant 2007), whereas this work concentrates on a strongly frictional system ($\delta \geq 1$). In low frictional systems, the relationship between velocity and sea surface elevation is described by the wave equation, whereas, in a frictionally dominated system, the relationship is defined by the diffusion equation.

The central result of this work is that tidal velocity and sea surface elevation are strongly damped upon entering into a shallow interconnected waterway. Tidal amplitude decreases rapidly with entrance into the inlets, with tidal phase increasing with increasing friction. Along- and cross-channel tidal velocities vary close to the entrances to the waterway. Along-basin flow is dominant within the channel, whereas cross-basin flows are more dominant over the shoals. Frictional effects dominate the dynamics within this interconnected system and Coriolis and local accelerations are small.

## 2. Model

The linear analytical model is based on a tidal model for a semi-enclosed basin described in Winant (2007). The model is defined as having an infinitely long coastline along the $x$ axis with a barrier separated from the coastline by a constant distance $B'$, the width of the basin. The barrier may have irregularly spaced inlets, although for this study only 2 inlets are considered, which are separated from each other by a length $2L'$. The depth across the inland waterway, between the coast and the barrier, is constant in the $x$ direction but has a narrow, deep channel in the cross-waterway direction of depth $h$ (Fig. 1). The cross-waterway depth is defined by an exponential function,

F1

$$h = 0.25 + 0.75 \exp^{-20y^2}. \tag{2}$$

This normalized depth is similar to the cross-waterway bathymetry in Florida's Intracoastal Waterway, where the maximum depth ($H'$) is 5 m in a narrow channel with wide shoals of 1-m depth. Positive $x$ direction runs along the channel with $x = 0$ at the south end of the channel and $x = 2$ at the north end of the channel. The $y$ axis extends across the channel with $y = 0$ along the center axis of the waterway. The solution of Winant (2007) is applied to one-half of the waterway assuming symmetry. Because the observed phase lag between the tide at the 2 inlets is negligible (~10 min), the solution is used for both sides of the waterway. The symmetric nature of the solution is appropriate in this case, given the strongly frictional nature of the inland waterway and the subsequent damping of the tidal signal. Between St. Augustine and Ponce de Leon Inlet, the Intracoastal Waterway has a half-basin length $L'$ of 50 km giving the nondimensional length parameter $\kappa = 1.0$ for the semidiurnal ($M_2$) tide. An initial estimate of the frictional parameter $\delta$ ranges from 0.8 to 1.7 (using $K'$ between 0.001 and 0.005 m$^2$ s$^{-1}$). In this work, $\kappa$ will be kept constant and $\delta$ will be varied.

In Winant (2007), complex amplitudes were used to approximate the periodic solutions of the tide such that

$$u = \mathrm{Re}[U(x,y,z)e^{-it}] \quad v = \mathrm{Re}[V(x,y,z)e^{-it}] \quad \text{and} \tag{3}$$

$$w = \mathrm{Re}[W(x,y,z)e^{-it}] \quad \eta = \mathrm{Re}[N(x,y)e^{-it}], \tag{4}$$

where $U$, $V$, and $W$ are the along, across, and vertical velocities in the basin and $N$ is tidal elevation. Winant (2007) uses the linearized momentum equations assuming shallow-water waves with a hydrostatic approximation in the vertical. A constant vertical eddy viscosity and negligible horizontal viscosities are also used. Boundary conditions on the bottom are no slip and at the surface are the kinematic and dynamic boundary conditions. At the open ends of the waterway, the tidal amplitude is assumed to be

$$N = 1 \quad \text{at} \quad x = 0, 2, \tag{5}$$

which indicates 0 phase lag between inlets for the tidal amplitude, given the complex nature of $N$. In the middle of the basin, at $x = 1$, the velocity normal to the boundary is assumed to be 0 ($N_x = 0$), meaning no transport occurs between the two adjacent basins at $x = 1$.

Assuming that depth or width depend only on $y$, the closed-form solution for the first-order fluctuation in sea level is

$$N^{(0)} = \frac{\cos[\kappa\mu(1-x)]}{\cos\kappa\mu}, \tag{6}$$

JOBNAME: JPO 00#0 2011 PAGE: 3 SESS: 8 OUTPUT: Thu Mar 24 14:31:36 2011 Total No. of Pages: 14
/ams/jpo/0/jpo4504



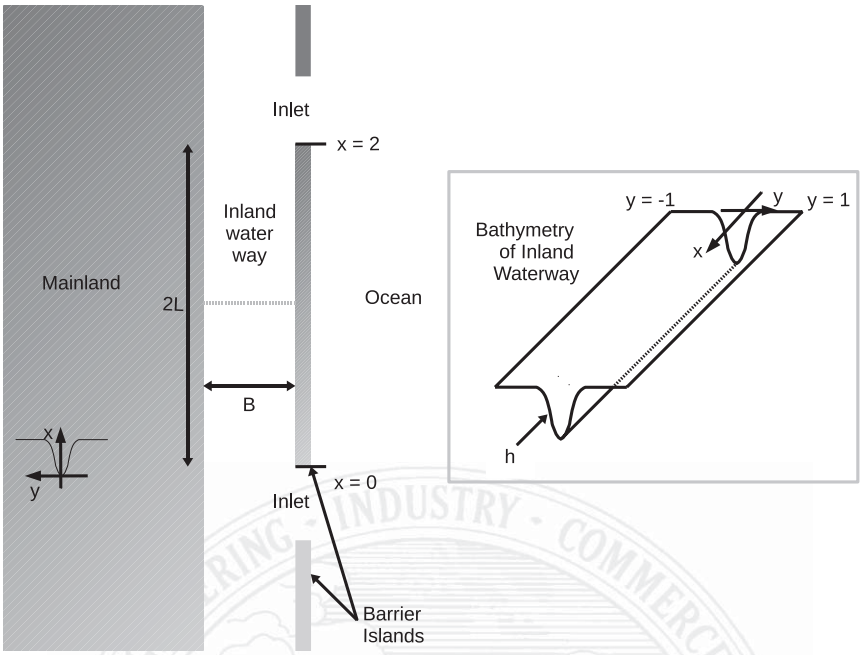


AU2 FIG. 1. Analytical model setup with 2 entrances (inlets) to an inland waterway. Dimensions of the model domain are $2L'$, $B'$, and $h'$. The dashed line at $x = 1$ denotes the location of the sea level minimum and 0 transport. The tide enters the 2 inlets synchronously at $x = 0$ and $x = 2$. The solution of sea surface elevation and transport velocity of the tidal signal is calculated between the 2 inlets.

where

$$\mu = \frac{\kappa}{\sqrt{\langle M_0 \rangle}}, \tag{7}$$

where the angle brackets denote a lateral average such that

$$\langle M_0 \rangle = \int_0^1 M_0 \, dy. \tag{8}$$

The definition of $M_0$ is $M_0 = (f^2 Q_0^2 / P_0) - P_0$, where $P_0$ and $Q_0$ are complex functions of $f$, $\delta$, and $h$. When friction is very low and $\delta$ goes to 0, both $P_0$ and $Q_0$ tend to $h/(f^2 - 1)$. Integrating the local velocities in depth gives horizontal transport velocities ($[\cdot]$) which in the along- and cross-channel directions are

$$[U] = -\frac{iN_x^{(0)} M_0}{\kappa^2} \quad \text{and} \tag{9}$$

$$[V] = \frac{iN_{xx}^{(0)} G}{\kappa^2}, \tag{10}$$

where $G = \int_0^y (M_0 - \langle M_0 \rangle)\, dy'$. The full derivation of the equations and full form of $P_0$ and $Q_0$ can be found in Winant (2007).

### a. *Sea level fluctuations* $N^{(0)}$

When the frictional parameter $\delta$ equals 1, the sea surface elevation $N^{(0)}$ is independent of $f$ as the parameters in Eq. (6) approach values that do not depend on $f$, as in Winant (2007). The phase and amplitude of $N^{(0)}$ are shown in Fig. 2 for both semidiurnal ($M_2$) and F2 diurnal ($K_1$) tidal frequencies. In these cases, the length of the basin is approximately equal to and less than one-quarter of the tidal wavelength ($\kappa = 1.0$ and 0.5) for the semidiurnal and diurnal tides, respectively. Thus, maximum tidal amplitudes are expected in the middle of the basin when $\delta < 1$ (Winant 2007), representative of tidal amplification with low friction. However, for $\delta = 1$, the amplitude of the sea surface decreases toward the middle of the waterway and then increases slightly, as observed in Winant (2007). For all cases with greater friction ($\delta > 1$), the tidal amplitude decreases exponentially upon entrance into the basin and does not change when $f$ is varied. For $\delta = 2$, $N^{(0)}$ at $x = 1$ is 0.03 of the amplitude at the entrance of the basins. For $\delta > 4$, the amplitude at $x = 1$ approaches 0.

When $\omega'$ decreases from the semidiurnal to the diurnal frequency, $\delta$ increases by a factor of $\sqrt{2}$, from Eq. (1). Therefore, the change in amplitude from the semidiurnal to the diurnal signals is similar to changes from lower to higher friction. The amplitude of the diurnal

JOBNAME: JPO 00#0 2011 PAGE: 4 SESS: 8 OUTPUT: Thu Mar 24 14:31:36 2011 Total No. of Pages: 14
/ams/jpo/0/jpo4504





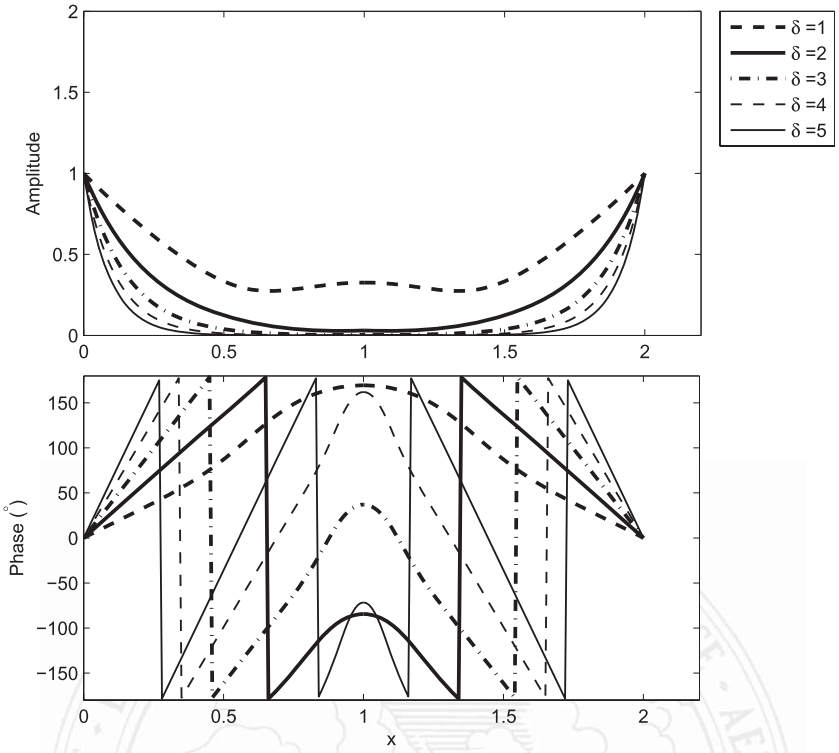


(a) Semi-Diurnal, $\kappa = 1.0,\ f = 0$

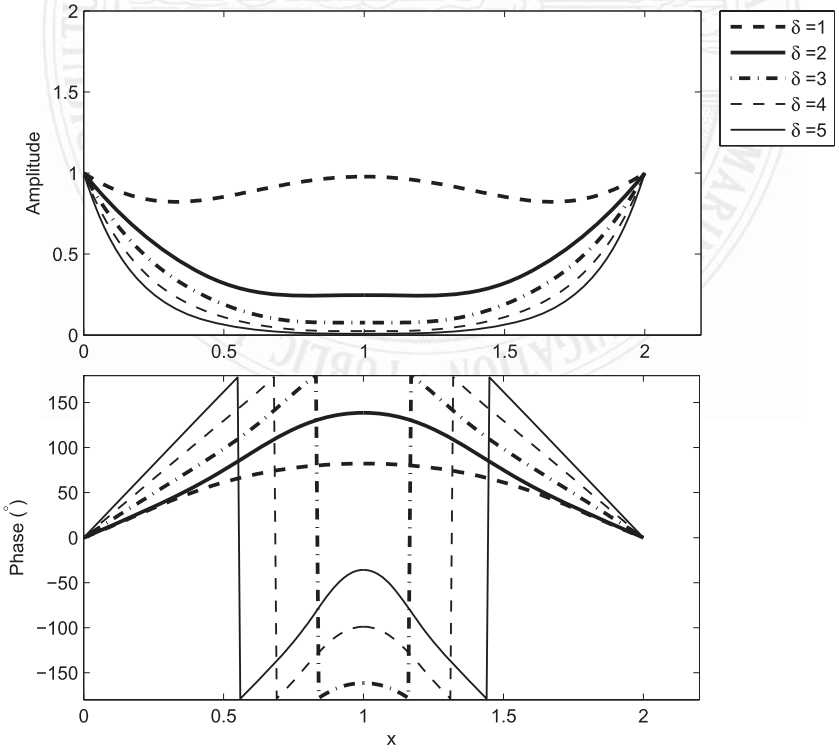


(b) Diurnal, $\kappa = 0.5,\ f = 0$

FIG. 2. Sea surface elevation $N^{(0)}$ amplitude and phase as calculated from the model for high values of friction, ranging from $\delta = 1$ to 5 for (a) the semidiurnal and (b) diurnal tides.

JOBNAME: JPO 00#0 2011 PAGE: 5 SESS: 8 OUTPUT: Thu Mar 24 14:31:36 2011 Total No. of Pages: 14
/ams/jpo/0/jpo4504



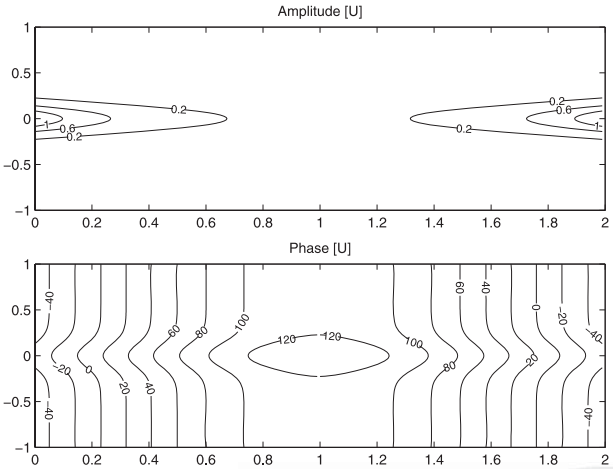


FIG. 3. (top) Amplitude and (bottom) phase of the along-channel transport $[U]$ from the analytical model with $\delta = 1.5$, $\kappa = 1.0$, and $f = 0$ for the semidiurnal tide.

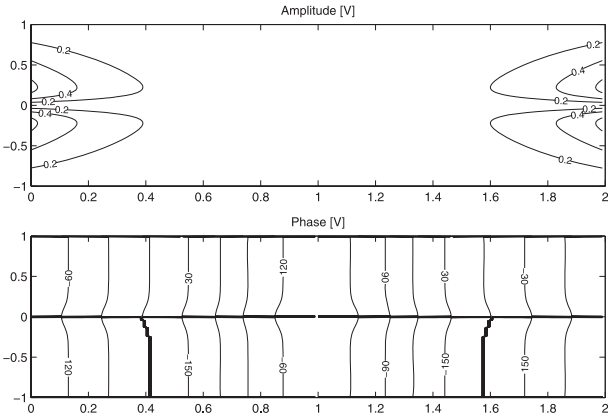


FIG. 4. As in Fig. 3, but for the cross-channel transport [V].

signal for $\delta = 1$ decreases from the entrances at $x = 0$ and 2 and then increases toward the midpoint at $x = 1$. As $\delta$ increases above 2, the amplitude of the tidal signal attenuates more quickly. The tidal amplitude decays more slowly than the semidiurnal tide. For large $\delta$, the equation determining the flow between the 2 inlets is dominated by pressure gradient and friction, and neither Coriolis nor local accelerations are important in the along-channel dynamics.

Phase increases from 0 at $x = 0$ with along-channel distance to the midpoint of the basin, where the phases then decrease back to the original input tidal phase (0 at $x = 2$). This is consistent with a tidal wave propagating along the basin from both sides ($x = 0$ and $x = 2$) toward $x = 1$. As friction increases ($\delta > 1$), the phase difference between the entrance and midpoint of the waterway also increases. This indicates that the tide propagates more slowly as friction increases and the peak from the entrance will not be felt at $x = 1$ until a longer time than for lower frictional values. With increasing friction, the governing differential equation changes from a wave equation to a diffusion equation. The wave equation indicates that the phase speed would be independent of friction, whereas the diffusion equation would make the phase speed dependent on friction. For $\delta = 1$, the phase change between the entrance and the midpoint of the basin is 170°. For the semidiurnal tide, this indicates a lag of 5.9 h between the high tide at the entrance and that at $x = 1$, whereas, for the diurnal tide, the lag between the entrance and $x = 1$ is 82.25° (5.5 h).

### b. *Transport velocities*

Transport velocity $[U]$ along the basin is symmetric across the basin with highest amplitudes in the channel and lowest over the shoals (Fig. 3). As the tide enters the basin from both inlets, the majority of the tidal energy enters through the deep narrow channel. Because of high friction ($\delta = 2$ in this case), the along-channel transport decreases in the channel as it approaches the midpoint of the waterway. The phase change in the channel is very small compared with that on the shoals. However, it does change with distance along the channel from positive (at the entrance) to negative inside the basin. The along-channel transport velocity responds more quickly on the shoals than in the channel because there is less inertia in shallower flow, and shoal transport leads transport velocity in the channel (Fig. 3).

The magnitude of the lateral transport $[V]$ is weaker than the along-channel transport with maxima occurring on the shoals, localized at the entrance to the basin (Fig. 4). The phases on each side of the channel are opposite (constant 180° difference); indicating flow toward the shoals during flood and off the shoals (toward the channel) during ebb. The amplitude and phase indicate that there is transport of water to the shoals as the tide enters through the channel. However, proceeding farther into the basin, the amplitude of $[V]$ decreases. Combined with $[U]$, mixing and transport of water (flushing) to and from the shoals may only be localized to an area near the entrance to the waterway as observed by Smith (1983).

### c. $N^{(0)}$ *and* [U]*: Phases*

Given a dynamically wide, frictionless basin, when the length of the basin is greater than one-quarter of the tidal wavelength ($\kappa \geq 1$), a node exists. On the basin side of this node, currents lead sea surface elevation by −90°, whereas, on the other side of the node, the lead is 90°. When the length of the basin decreases to less than one-quarter of the tidal wavelength ($\kappa < 1$), the node disappears and currents lead elevation by 90°. When friction increases, however, the phase relationship between $N^{(0)}$ and $[U]$ is no longer 90°. The deviation from 90° is discussed next as friction increases from $\delta = 1$ to 5.

JOBNAME: JPO 00#0 2011 PAGE: 6 SESS: 8 OUTPUT: Thu Mar 24 14:31:37 2011 Total No. of Pages: 14
/ams/jpo/0/jpo4504



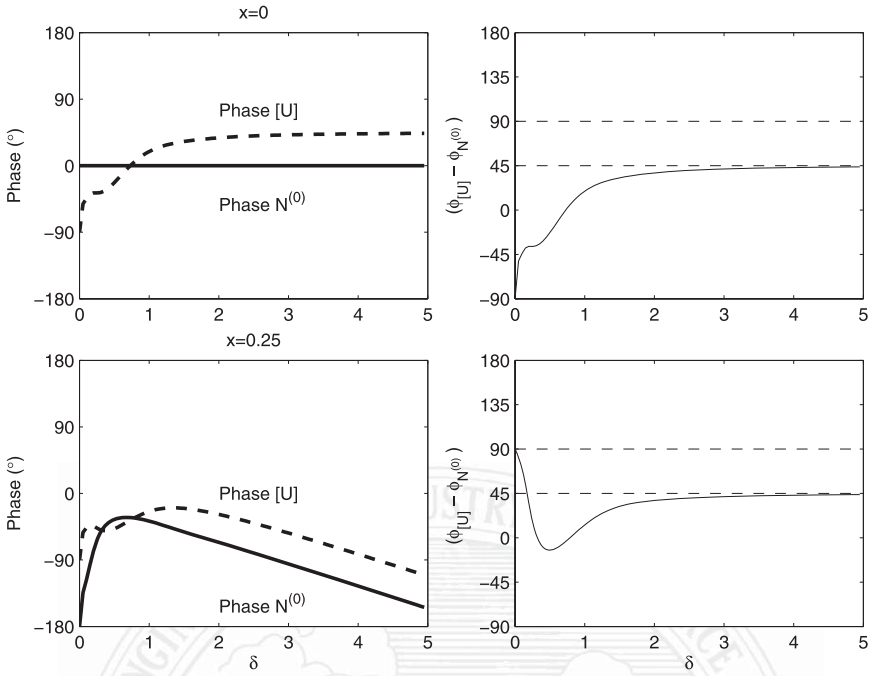


FIG. 5. (left) Phases of sea surface elevation $N^{(0)}$ and along-channel transport $[U]$ and (right) the phase difference between $N^{(0)}$ and $[U]$ for various values of $\delta$ ranging from 1 to 5 for the semidiurnal tide with $\kappa = 1.0$ and $f = 0$: $x =$ (top) 0.00 and (bottom) 0.25.

The phase of $N^{(0)}$ is set to be 0 at the entrances to the waterway [$N^{(0)} = 1$], and the phase of $[U]$ at the entrance is related to the nondimensional length of the basin. These phases are plotted at $x = 0$ and $x = 0.25$ along the middle of the basin (at $y = 0$) for both semidiurnal and diurnal tidal frequencies (Figs. 5, 6). The phase of $[U]$ at $x = 0$ varies as $\delta$ increases while, given the boundary condition at the entrance, the phase of $N$ remains 0. When $\delta = 0$ for the semidiurnal tide, currents lead sea surface elevation by $-90°$ at the entrance of the basin because $\kappa = 1.0$ and a node would be expected given the tidal wave oscillation in a frictionless basin (Fig. 5). However, as friction increases, the phase difference approaches 45° but not linearly. Small changes in friction between $\delta = 0$ and 2 result in a significantly different phase lag between sea surface elevation and velocity. Above $\delta = 2$, the phase lag approaches 45° more asymptotically than for $\delta < 2$. The importance of friction in modifying the tidal propagation (and subsequent node) is highlighted as the currents change from a phase lag of $-90°$ to 45° over relatively small changes in frictional parameter ($\delta = 0$–2).

Farther along the basin at $x = 0.25$, the phase of both sea surface elevation and velocity vary with $\delta$ (Fig. 5). The phase lag between elevation and velocity asymptotically approaches 45°, for $\delta > 2$ with the minimum phase lag occurring at $x = 0.5$ of $-12.6°$. For a particular inlet with a frictional value of $\delta = 1$, the phase lag between sea surface elevation and velocity will vary depending on the sampling location within the inlet. For $\delta = 1$ at $x = 0$, the phase lag will be 19°, whereas, at $x = 0.25$, the phase lag will be 13°.

Phase lags for the diurnal signal (Fig. 6) vary from 90° to 45° differently than for the semidiurnal signal because $\kappa < 1$. At $x = 0$, the phase of the transport velocity increases from $\delta = 0$ to 2, at which point it becomes steady at approximately 45°. The minimum in phase lag between $[U]$ and $N^{(0)}$ occurs for $\delta = 1$ at 24°. Farther along the inland waterway, at $x = 0.25$, the phase lag decreases from 90° to 45° asymptotically approaching 45° for $\delta > 2$.

Phase lags between transport velocity and elevation ranging from $-90$ to 90°, as described in Friedrichs (2010), are captured by this analytical model. In the case with a highly frictional basin with two openings, the phase lag is found to be dependent on frictional effects. In a more general case, depending on the basin length, lateral depth variations, and tidal frequency, the phase lag between transport velocity and sea surface elevation will vary with distance along the basin.

## 3. Observations

In situ observations are used to determine whether the tidal behavior from the inland waterway of Florida's

JOBNAME: JPO 00#0 2011 PAGE: 7 SESS: 8 OUTPUT: Thu Mar 24 14:31:37 2011 Total No. of Pages: 14
/ams/jpo/0/jpo4504



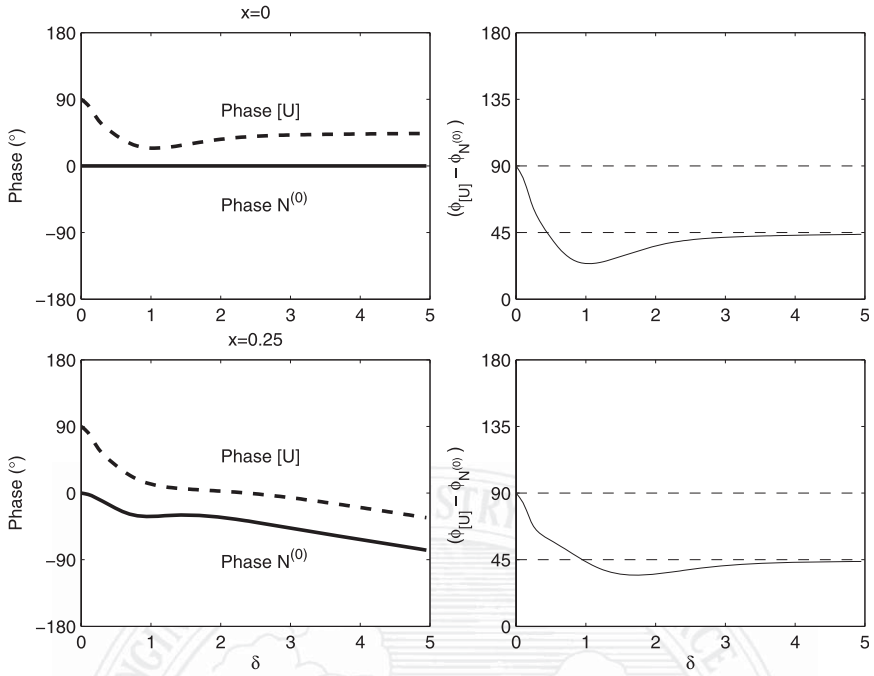


FIG. 6. As in Fig. 5, but for the diurnal tide with $\kappa = 0.5$ and $f = 0$.

Intracoastal Waterway matches that predicted by the analytical model. Florida's Intracoastal Waterway is a dredged waterway extending along the eastern coast of Florida. The mean width of the Intracoastal Waterway is 55 m, with expansive shoals (1-m depth) and a maximum depth of 5 m (Smith 1983; Kenworthy and Fonseca 1996) in a narrow navigational channel. Ponce de Leon Inlet and St. Augustine Inlet are two of 19 coastal inlets connecting the Intracoastal Waterway to the Atlantic Ocean (Dean and O'Brien 1987). Tidal flows within these two inlets are forced by the semidiurnal ($M_2$) tide and more weakly by the diurnal ($K_1$) tide, with typical tidal currents exceeding 1 m $s^{-1}$. Tidal flows entering through these inlets will interact with the variable bathymetry and also possibly with the tidal signal within the waterway as a result of the open communication between the inlets.

A total of nine pressure records were used to determine the tidal amplitude and phase along the Intracoastal Waterway. Six pressure sensors, developed for Kennedy et al. (2010), were deployed over 14 days from 3 to 17 December 2009 at various locations between St. Augustine Inlet and Ponce de Leon Inlet (Fig. 7). Surface elevation was recorded at bursts of 60 s, every 14 min, sampling at 5 Hz. The data were averaged over each sampling period leaving one ensemble average every 15 min.

The harmonic constituents from three other pressure (and two velocity) records, which were deployed prior to December 2009, were obtained using T_TIDE without inference (Pawlowicz et al. 2002). Pressure and velocity records were reconstructed using the harmonic constituents, without inference, for the sampling period between 3 and 17 December 2009. The first reconstructed series was pressure from sensor 8, deployed from 13 December 2009 to 9 January 2010 at a location south of St. Augustine Inlet (sensor 8; Fig. 7). The two other sensors were from two acoustic Doppler current profilers (ADCPs) deployed at the mouths of Ponce de Leon and St. Augustine Inlets. These ADCPs were deployed from January to March 2008 (Ponce de Leon Inlet, depth of 8 m) and from July to September 2008 (St. Augustine, depth of 15 m) in the deepest part of each inlet. Each ADCP recorded pressure and profiles of velocity. Ensemble averages of 0.5-m bins were recorded at a ping rate of 1.5 s with 400 pings per ensemble. Current velocities were rotated to be aligned with the principal axis of maximum variance such that positive along-channel velocity was directed into the inlet and positive across-channel velocity was southward.

Two more ADCPs were moored at Port Orange, Florida (between pressure sensors 2 and 3; Fig. 7), from 3 to 17 December 2009. A 600-kHz ADCP was moored in the navigation channel at 5-m depth, whereas the second ADCP was moored on the eastern bank in a hole (4 m). Both ADCPs measured ensemble averages of 0.5-m bins at a ping rate of 1.2 s with 400 pings per ensemble. Data from the channel were rotated to the principal axis of maximum variance (by 76°) such that

JOBNAME: JPO 00#0 2011 PAGE: 8 SESS: 8 OUTPUT: Thu Mar 24 14:31:37 2011 Total No. of Pages: 14
/ams/jpo/0/jpo4504



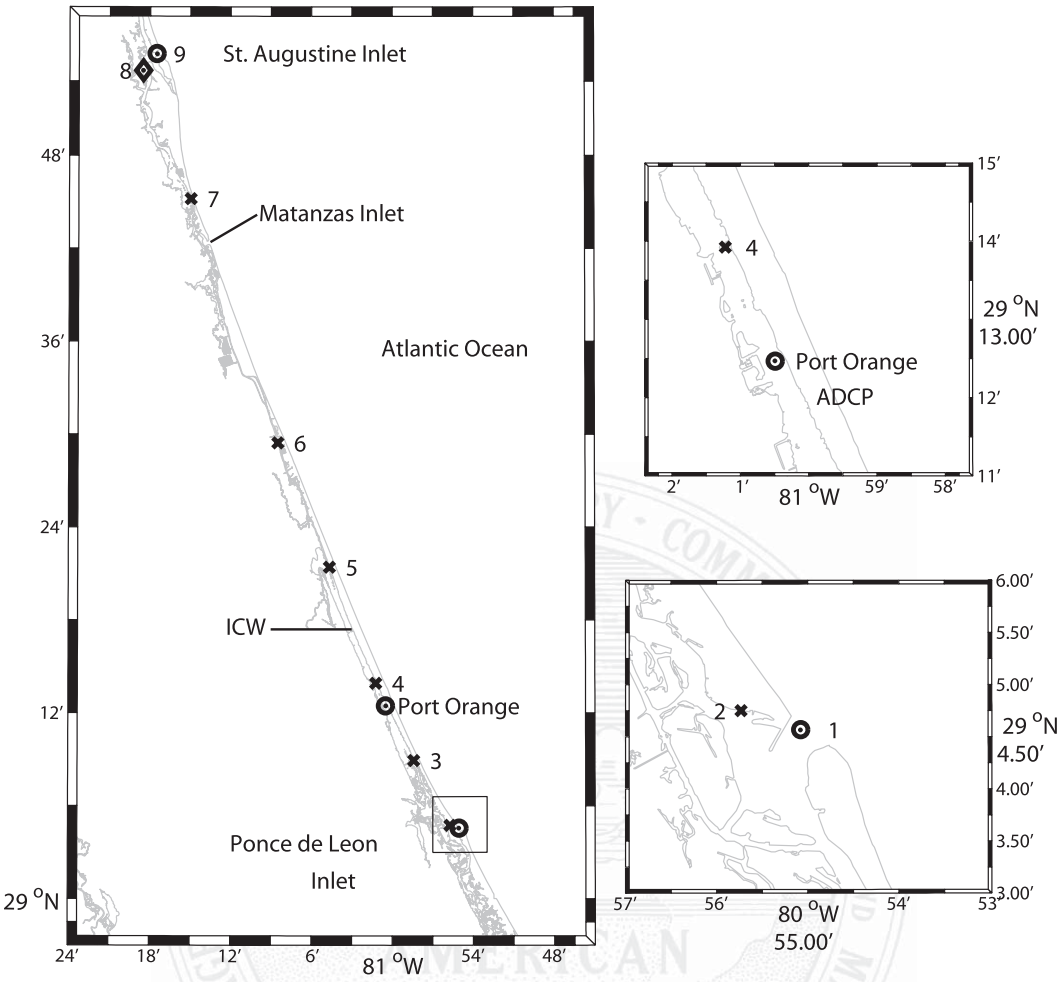


FIG. 7. Maps showing locations of 6 pressure sensors (×) moored in the Intracoastal Waterway from 3 to 17 Dec 2009. Sensors whose harmonic constituents were used to reconstruct pressure and velocity signals are the 2 ADCPs at the mouths of St. Augustine and Ponce de Leon (circles) as well as pressure sensor 8, south of St. Augustine Inlet (diamond). All numbered stations are used in the sea surface elevation amplitude and phase calculations. Transport velocities and pressure were used from the ADCPs moored for at least 1 fortnightly tidal cycle (circles).

positive along-channel velocity was northward and positive across-channel velocity was eastward. The second ADCP was not deployed exactly on the shoal but in a hole in the shoal region, and therefore these data are not discussed in this paper.

All pressure and velocity records were bandpass filtered, isolating the semidiurnal (1–18 h) and diurnal (20–36 h) components. The amplitude and phase change of the pressure signals along the Intracoastal Waterway were then found using a Hilbert empirical orthogonal eigenfunction (Hilbert EOF) analysis. The Hilbert EOF analysis captures the change in amplitude and phase of a signal that has the same frequencies but different phases of that frequency (Horel 1984; Merrifield and Guza 1990; Von Storch and Zwiers 2001; Emery and Thomson 2004; Hannachi et al. 2007). In contrast to the traditional EOF method, Hilbert EOFs return both the amplitude and phase of a complexified dataset relative to the first input signal (sea surface elevation or velocity), which is assigned zero phase. For this work, all phases are thus relative to the southernmost inlet, Ponce de Leon Inlet. The 6 pressure sensors (sensors 2–7) had different time stamps associated with the start time of the sensor, and this difference was accounted for by subtracting the appropriate phase shift (in time) from the phase output from the Hilbert EOF analysis for each of those sensors. The phase lag between the elevation and along-channel velocity were also found using a Hilbert EOF analysis.

### *a. Sea level fluctuations $N^{(0)}$*

Pressure records collected along the Intracoastal Waterway were compared with model results (Fig. 8). Like F8

JOBNAME: JPO 00#0 2011 PAGE: 9 SESS: 8 OUTPUT: Thu Mar 24 14:31:37 2011 Total No. of Pages: 14
/ams/jpo/0/jpo4504





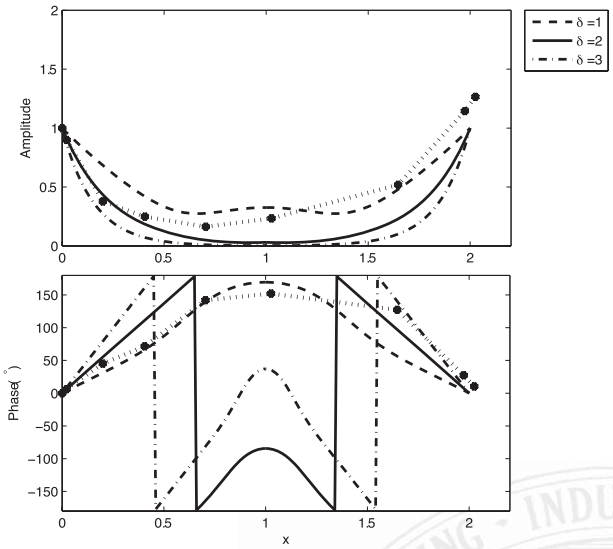


(a) Semi-Diurnal, $\kappa = 1.0$, $f = 0$

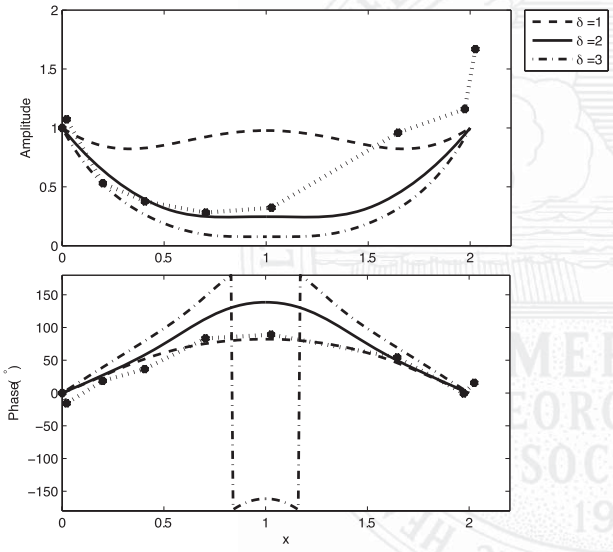


(b) Diurnal, $\kappa = 0.5$, $f = 0$

FIG. 8. Observations of sea surface elevation $N^{(0)}$ amplitude (solid circles) and phase (dotted line) between Ponce de Leon Inlet ($x = 0$) and St. Augustine Inlet ($x = 2$): (a) semidiurnal and (b) diurnal tide. Model data are shown below for those $\delta$ that match with the observed results.

the model results, the tidal amplitude decreases from both openings of the channel toward the center point ($x = 1$). The phase increases with distance along the channel from both inlets, consistent with the model results. The phase lag from $x = 0$ and $x = 1$ is 152° and 89° for the semidiurnal and diurnal signals, respectively. This corresponds to a 5.2- and 5.9-h phase lag between the inlets and the midpoint of the inland waterway. Using the frictional parameter of $\delta = 1.5$ (from the best fit between observations and the model results) and a maximum depth of 5 m in Eq. (1), the constant eddy viscosity is $K' = 0.004\ \mathrm{m^2\ s^{-1}}$. Using this eddy viscosity with the diurnal tidal frequency $\omega'$ gives $\delta = 2.1$, which corresponds to the observed fit between the model result and observations for the diurnal tide.

### b. *Transport velocity* [U]

The transport velocity is defined in this context as the vertically integrated velocity. The tidal amplitude and phase of the transport velocity within the Intracoastal Waterway was obtained from the Hilbert EOF analysis of depth-averaged nondimensionalized velocities from each of the three deployed ADCPs and using the pressure from Ponce de Leon Inlet as the reference pressure. All first mode amplitudes from the Hilbert EOF were normalized to the first mode amplitude of the pressure sensor.

The amplitude of $[U]$ decreases toward the center of the basin (Fig. 9). At $x = 0$, the semidiurnal amplitude of the transport is less than at $x = 2$, indicating an imbalance in the input tidal signal from each of the locations. The diurnal transport velocity amplitude is also overpredicted by the model at both entrances, but its shape resembles the observations, showing a decrease in transport velocity with distance into the basin. F9

The phase of the transport velocity varies from negative close to the mouths of the waterway to positive at the station within the Intracoastal Waterway at Port Orange for both the semidiurnal and diurnal transport velocities. The observations are in agreement with the phases from the model where a smaller phase lag in the diurnal signal at $x = 1$ was observed compared with the semidiurnal signal.

### c. $N^{(0)}$ *and* [U]*: Amplitudes*

To compare the change in amplitudes of both velocity and sea surface elevation, the ratio of $[U]$ and $N^{(0)}$ was compared between the model and the observations. Model results of the along-channel amplitudes of $N^{(0)}$ and $[U]$ and the ratio of the two are shown in Fig. 10. The ratio of the standard deviation between along-channel transport velocity and surface elevation are calculated at all current meter locations. The accuracy of the pressure sensor from the ADCP is less than the change in water level and therefore the pressure from sensor 3 is used as the pressure from the Port Orange ADCP. The ratios of the observed standard deviations were compared to the dimensionalized model results from $\delta = 1.5$, $\kappa = 1.0$, and $f = 0$. To obtain dimensionalized values from the model, the model ratios were multiplied by the tidal frequency $\omega'$ and the channel length $L'$ given by F10

$$\frac{[U]_{\mathrm{obs}}}{\eta_{\mathrm{obs}}} = \frac{[U]_{\mathrm{model}}}{N^{(0)}_{\mathrm{model}}}\omega' L'. \tag{11}$$

JOBNAME: JPO 00#0 2011 PAGE: 10 SESS: 8 OUTPUT: Thu Mar 24 14:31:37 2011 Total No. of Pages: 14
/ams/jpo/0/jpo4504



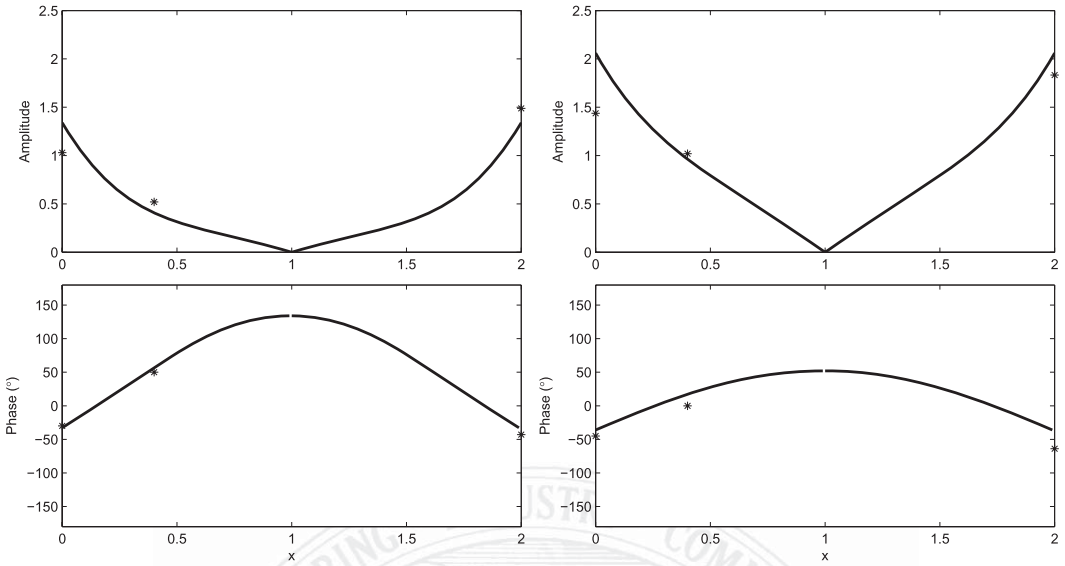


FIG. 9. (top) Amplitude and (bottom) phase of the observed (asterisks) and modeled (solid line) along-channel transport $[U]$ for (a) semidiurnal ($\delta = 1.5$, $\kappa = 1.0$) and (b) diurnal ($\delta = 2$, $\kappa = 0.5$) tides with $f = 0$.

From the current meter moored at Port Orange (between sensors 2 and 3), the ratios from both the observed semidiurnal and diurnal tides are in close agreement with the model predictions (Table 1). The ratio of $[U]_{\text{model}}$ over $N^{(0)}_{\text{model}}$ increases to a maximum at $x = 0.7$ and 1.3 and $x = 0.5$ and 1.5, decreasing to zero at $x = 1$ for the semidiurnal and diurnal signals, respectively (Fig. 10).

At St. Augustine, the semidiurnal tide ratio is much larger than the model predicts. This inconsistency is likely related to the sensitivity of velocity to accurate bathymetry in the along-and cross-channel directions, whereas sea surface elevation is not as dependent on accurate bathymetry. The diurnal observed ratios follow the model output, which shows larger predicted and observed amplitude ratios at Port Orange ($x = 0.3$).

### *d. $N^{(0)}$ and [U]: Phases*

At all three mooring locations, velocity leads the sea surface elevation. The change in the spatial (local) lead of currents over elevation was calculated from the Hilbert EOF analysis of the along-channel transport with pressure (normalized by the standard deviation of the currents over the pressure). For the semidiurnal tide, with $\delta = 1.5$, the phase lead of currents over sea surface elevation is consistent with the model results (Fig. 11). The semidiurnal phase difference is less than 45° near the entrances of the inland waterway, as observed in Fig. 5. Model predictions indicate that the phase difference will only reach 90° close to the middle of the waterway at $x = 1$ with the phase differences staying constant until $x = 0.45$ and $x = 1.6$. The model output predicts that the phase difference between elevation and velocity for the diurnal signal is 45° at the mouths of the inlet and 90° at $x = 1$. The observed diurnal phase differences at Ponce de Leon Inlet ($x = 0$) and Port Orange ($x = 0.3$) are similar to those predicted by the model. However, at St. Augustine Inlet ($x = 2$), the observed phase difference is much larger than predicted by the model (90°), closer to a standing wave for the diurnal tide. Without additional information, the observed phase difference is likely due to influences of Matanzas inlet, which will be discussed in the next section.

## 4. Discussion

Analytical model results and observations of sea surface elevation and tidal flow demonstrate that the tide, synchronous between Ponce de Leon Inlet and St. Augustine Inlet, enters at both inlets and quickly attenuates within the Intracoastal Waterway. The tide diffuses through the inland waterway, rather than propagates, because of frictional effects. The eddy viscosity is estimated to be 0.004 $m^2\ s^{-1}$, given the best fit $\delta$ between the observations and the model for the semidiurnal and diurnal tides. Therefore, the shallow depth accounts for the strong attenuation of the tide with distance along the inland waterway. LeBlond (1978) came to the same conclusion in developing a simple diffusive model for tidal rivers of much larger scale such as the Fraser and St. Lawrence Rivers.

JOBNAME: JPO 00#0 2011 PAGE: 11 SESS: 8 OUTPUT: Thu Mar 24 14:31:38 2011 Total No. of Pages: 14
/ams/jpo/0/jpo4504





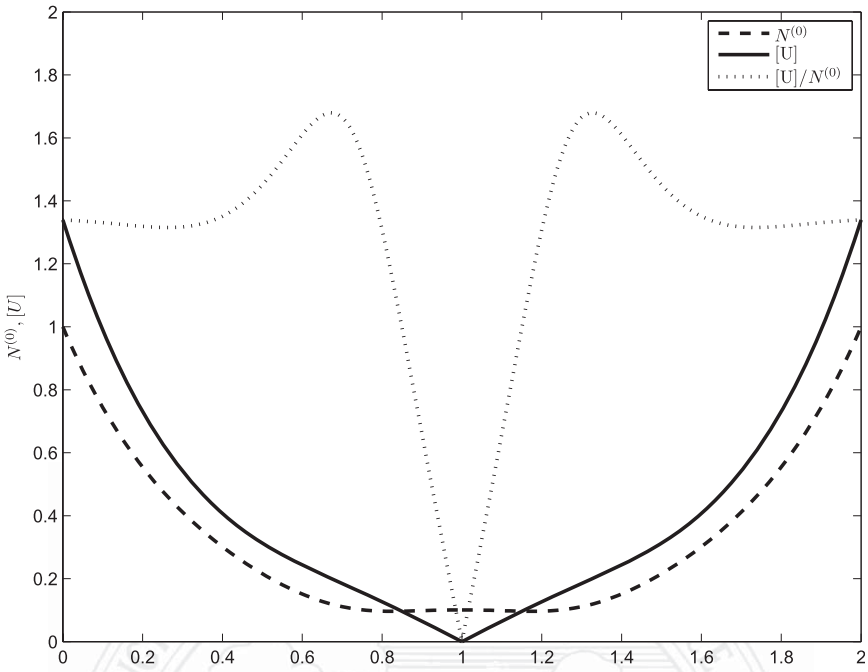


(a) Semi-Diurnal, $\delta = 1.5$, $\kappa = 1.0, f = 0$

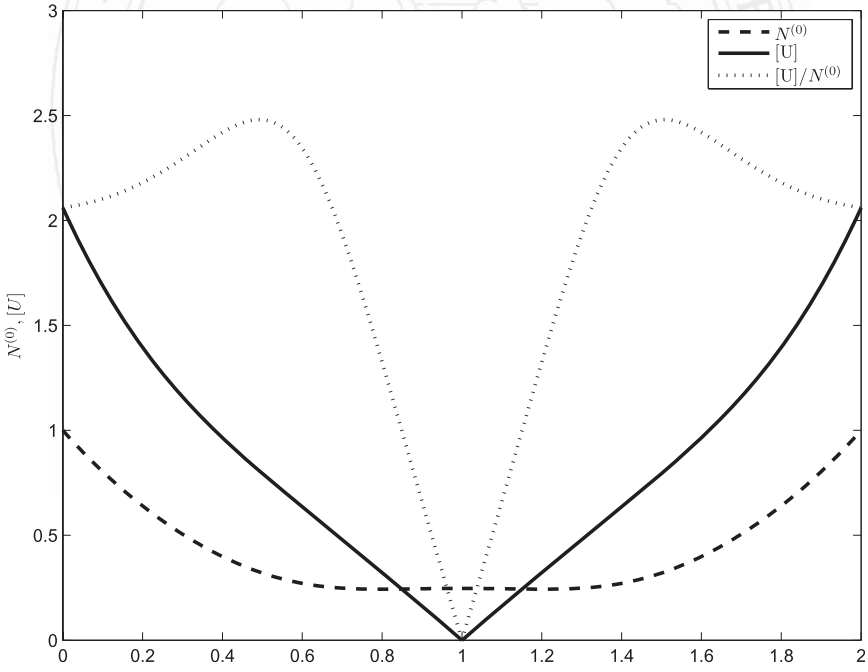


(b) Diurnal, $\delta = 2$, $\kappa = 0.5, f = 0$

FIG. 10. Amplitudes of modeled $N^{(0)}$ and $[U]$ and the ratio of $N^{(0)}/[U]$: (a) semidiurnal and (b) diurnal tide. The amplitude of the observed ratio compares well with the model ratio, in dimensional units (see Table 1). To convert to dimensional units (so as to compare with results in Table 1), nondimensional ratios here must be multiplied by $\omega' L'$ for each semidiurnal and diurnal frequency. Here, $x = 0.3$ represents the location of the ADCP mooring at Port Orange.

JOBNAME: JPO 00#0 2011 PAGE: 12 SESS: 8 OUTPUT: Thu Mar 24 14:31:38 2011 Total No. of Pages: 14
/ams/jpo/0/jpo4504





TABLE 1. Ratio of $[U]/N^{(0)}$ from ADCPs moored at 3 locations in Florida's Intracoastal Waterway compared with dimensionalized ratios from the model from $\delta = 1.5$ and $\kappa = 1.0$ for the semidiurnal tide and $\delta = 2$ and $\kappa = 0.5$ for the diurnal tide. Rotation is not considered ($f = 0$).

| | Mooring | $U_{obs}/\eta_{obs}$ | $U_{model}/N_{model}$ |
|---|---|---|---|
| Semidiurnal | Ponce de Leon | 16.6 | 9.4 |
| | Port Orange | 14.6 | 9.3 |
| | St. Augustine | 41.6 | 9.4 |
| Diurnal | Ponce de Leon | 8.0 | 7.5 |
| | Port Orange | 8.5 | 8.3 |
| | St. Augustine | 7.4 | 7.5 |

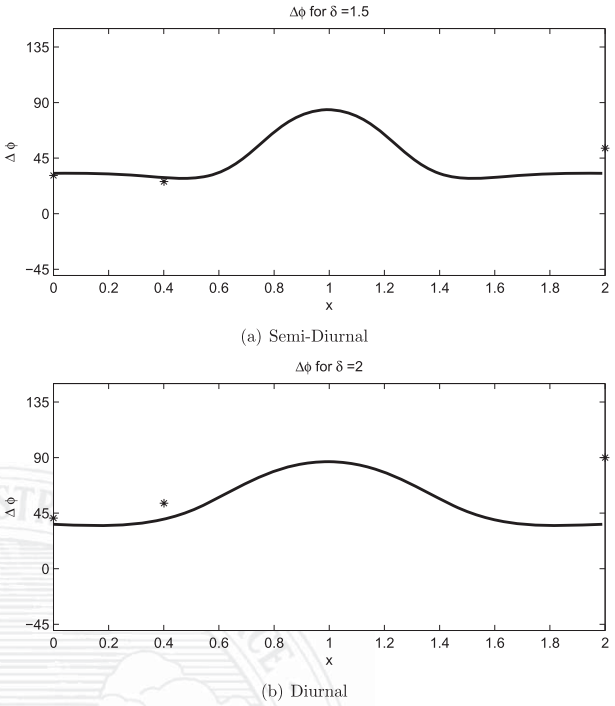


FIG. 11. Modeled (solid line) and observed (asterisks) local phase difference between velocity and sea surface elevation at the three ADCP locations along the inland waterway: (a) semidiurnal and (b) diurnal tide.

The tide in the Intracoastal Waterway along the east coast of Florida is prescribed, at irregular intervals, by the open ocean tide. The dynamics in the Intracoastal Waterway are determined by a balance between friction and pressure gradient. When a characteristic length in the $x$ direction, separating the two inlets, is large such that tidal amplitudes and velocities attenuate to zero, there will be no flushing around the middle region of the waterway. Similar observations by Smith (1983) showed that there was relatively rapid flushing near the inlet, but with little to no net movement of water in the interior of the Intracoastal Waterway. Smith (1983) suggested that because of the lack of tidal flushing, low-frequency variations would be more important in the interior of the waterway, in terms of flushing times. From our observations between Ponce de Leon and St. Augustine Inlet, the water level variations do not reach 0 (0.2 m); however, predicted transport velocity goes to 0. This indicates that minimal to no flushing is occurring at the midpoint between the two inlets.

The tidal velocity strength along the basin is determined by the lateral dimensions of the basin. In our case, the channel is very narrow and deep with respect to the shoals. As the tide enters through the inlets, the tidal transport follows the channel and the tidal velocity decreases quickly over the shoals. The amplitude of the surface elevation, however, is constant laterally (in $y$), varying only along $x$. Because the flow spreads out laterally over the shoals close to the entrance of the channel (Fig. 4), flushing will only occur as a result of this local mixing. Studies of the interconnectivity of these basins on the tidal evolution within the waterway have shown the existence of mean flows as a result of tidal and water level differences along the waterway (van de Kreeke and Dean 1975; Smith 1983; Liu 1992; Huang et al. 2002). Modeling from van de Kreeke and Dean (1975) showed that residual flows resulted from differences in tidal amplitudes and phases between two inlets. Although mean flows would effectively increase flushing and have not been considered in this model, flushing as a result of tidal processes is still likely important at inlet mouths. Further simplifications of the bathymetry in the model at the inlet mouths will underestimate the different amount of tidal flushing occurring between the two inlets. Because the cross-sectional area (and resulting tidal prism) is larger in St. Augustine Inlet than in Ponce de Leon Inlet (Walton and Adams 1976), enhanced tidal flushing is likely occurring in St. Augustine Inlet relative to Ponce de Leon Inlet (O'Brien 1931, 1969).

Inconsistency in the comparisons between the model and observations in the region between $x = 1$ and $x = 2$, close to St. Augustine Inlet, has been attributed to two likely sources. The first is the interaction of tidal signals from Matanzas Inlet, which is a narrow shallow, undredged channel 24 km south of St. Augustine Inlet. Although the tidal signal is likely damped through its long, sinuous entrance into the Intracoastal Waterway, given the results shown from the observations, the increase in tidal amplitude observed in pressure sensors between $x = 1$ and $x = 2$ is likely a result of the tide from Matanzas Inlet. Although the tidal signal is damped once reaching the entrance to the Intracoastal Waterway (at $x = 1.5$), the influence of this tidal signal can be seen in Fig. 8 from $x = 1$ to $x = 2$ because the tidal amplitude is larger than from the model. The phase of the semidiurnal signal beyond $x = 1$ indicates a decrease

JOBNAME: JPO 00#0 2011 PAGE: 13 SESS: 8 OUTPUT: Thu Mar 24 14:31:38 2011 Total No. of Pages: 14
/ams/jpo/0/jpo4504





in propagation speed as a result of the higher than expected phase, perhaps from the influence of Matanzas Inlet. The second explanation for the increased amplitude at St. Augustine is likely associated with the difference in mooring depth between both inlets. St. Augustine is a much wider and deeper inlet than Ponce de Leon Inlet, and the ADCP was moored at 15 m (compared with 8 m in Ponce de Leon Inlet). The tidal wave was under different frictional conditions because of different depths and was likely more damped when measured inside Ponce de Leon Inlet than in St. Augustine Inlet.

## 5. Conclusions

In a shallow inland waterway with openings to the adjacent ocean, the main tidal dynamics are driven by the balance between pressure gradient and friction. Observations of velocity and sea surface elevation are well described with an analytical model that uses the linearized equations of momentum. In highly frictional environments, such as Florida's Intracoastal Waterway, the tidal amplitude decays rapidly away from both openings. As friction increases, decay of the tidal amplitude occurs closer to the entrances and the propagation of the tidal signal is slower.

Transport velocity follows the basin bathymetry, with strongest along-channel transport velocities in the channel. The shallow depth of the shoals allows for the shoals to react more quickly to tidal signals, and along-channel transport in the channel lags those on the shoals. Lateral transport at the entrances to the inland waterway is onto the shoals during flood tide and off the shoals during ebbs. This indicates localized mixing at the mouths of the inlets, decreasing toward the center of the inland waterway.

In a frictionless basin, the phase lag between sea surface and elevation is 90°, as expected in a co-oscillating tidal solution. However, the phase approaches 45° at high friction but tends to decrease below 45° for moderately high friction. The phase lag between sea surface elevation and current varies with location within the inland waterway and may increase to 90° at the center of the waterway. Overall, the model describes well the propagation and attenuation of the tide within an inland waterway.

*Acknowledgments.* The authors are extremely grateful to Uriah Gravois and Andrew Kennedy for the use of, help with programming, and setup of their pressure sensors. We also thank Vik Adams, Andrew Lapetina, and Chloé Winant for their assistance in the field setup and instrument retrieval and to James Kotas for allowing the use of his dock for multiple mooring deployments in Port Orange. Discussion with R. G. Dean helped in clarifying the effect of Matanzas inlet and varying inlet size, and the comments of two anonymous reviewers are greatly appreciated. AFW and AVL acknowledge support of NSF projects OCE-0726697 and OCE-0825876 as well as funding from the University of Florida Water Institute.

## REFERENCES

Dean, R. G., and M. P. O'Brien, 1987: Florida's west coast inlets: Shoreline effects and recommended action. University of Florida Coastal and Oceanographic Engineering Department Tech. Rep. UFL/COEL 87/018, XX pp. AU1

Emery, W. J., and R. E. Thomson, 2004: *Data Analysis Methods in Physical Oceanography*. 2nd ed. Elsevier, 638 pp.

Friedrichs, C., 2010: Barotropic tides in channelized estuaries. *Contemporary Issues in Estuarine Physics,* A. Valle-Levinson, Ed., Cambridge University Press, 27–61.

——, and O. Madsen, 1992: Nonlinear diffusion of the tidal signal in frictionally dominated embayments. *J. Geophys. Res.,* **97** (C4), 5637–5650.

——, and D. Aubrey, 1994: Tidal propagation in strongly convergent channels. *J. Geophys. Res.,* **99,** 3321–3336.

Hannachi, A., I. T. Jolliffe, and D. B. Stephenson, 2007: Empirical orthogonal functions and related techniques in atmospheric science: A review. *Int. J. Climatol.,* **27,** 1119–1152.

Hendershott, M. C., and A. Speranza, 1971: Co-oscillating tides in long, narrow bays; The Taylor problem revisited. *Deep-Sea Res. Oceanogr. Abstr.,* **18,** 959–980, doi:10.1016/0011-7471(71)90002-7.

Horel, J. D., 1984: Complex principal component analysis: Theory and examples. *J. Climate Appl. Meteor.,* **23,** 1660–1673.

Huang, W., H. Sun, S. Nnaji, and W. K. Jones, 2002: Tidal hydrodynamics in a multiple-inlet estuary: Apalachicola Bay, Florida. *J. Coastal Res.,* **18,** 674–684.

Kennedy, A. B., and Coauthors, 2010: Rapidly installed temporary gauging for hurricane waves and surge, and application to Hurricane Gustav. *Cont. Shelf Res.,* **30,** 1743–1752.

Kenworthy, W. J., and M. S. Fonseca, 1996: Light requirements of seagrasses *Halodule wrightii* and *Syringodium filiforme* derived from the relationship between diffuse light attenuation and maximum depth distribution. *Estuaries,* **19,** 740–750.

LeBlond, P. H., 1978: On tidal propagation in shallow rivers. *J. Geophys. Res.,* **83** (C9), 4717–4721.

Li, C., and A. Valle-Levinson, 1999: A two-dimensional analytic tidal model for a narrow estuary of arbitrary lateral depth variation: The intratidal motion. *J. Geophys. Res.,* **104,** 23 525–23 543.

Liu, J. T., 1992: The influence of episodic weather events on tidal residual currents: A case study at Sebastian Inlet, Florida. *Estuaries,* **15,** 109–121.

Merrifield, M. A., and R. T. Guza, 1990: Detecting propagating signals with complex empirical orthogonal functions: A cautionary note. *J. Phys. Oceanogr.,* **20,** 1628–1633.

O'Brien, M. P., 1931: Estuary tidal prisms related to entrance areas. *Civ. Eng.,* **1,** 738–739.

——, 1969: Equilibrium flow areas of tidal inlets on sandy coasts. *J. Waterw. Harbors.,* **95,** 43–52.

Pawlowicz, R., B. Beardsley, and S. Lentz, 2002: Classical tidal harmonic analysis including error estimates in MATLAB

JOBNAME: JPO 00#0 2011 PAGE: 14 SESS: 8 OUTPUT: Thu Mar 24 14:31:38 2011 Total No. of Pages: 14
/ams/jpo/0/jpo4504



using T_TIDE. *Comput. Geosci.,* **28,** 929–937, doi:10.1016/S0098-3004(02)00013-4.

Prandle, D., 2003: Relationships between tidal dynamics and bathymetry in strongly convergent estuaries. *J. Phys. Oceanogr.,* **33,** 2738–2750.

Smith, N. P., 1983: Tidal and low-frequency net displacement in a coastal lagoon. *Estuaries Coasts,* **6,** 180–189, doi:10.2307/1351510.

Taylor, G. I., 1921: Tidal oscillations in gulfs and rectangular basins. *Proc. London Math. Soc.,* **20,** 148–181.

van de Kreeke, J., and R. Dean, 1975: Tide-induced mass transport in lagoons. *J. Waterw. Harbors Coastal Eng. Div.,* **101,** 393–403.

Von Storch, H., and F. W. Zwiers, 2001: *Statistical Analysis in Climate Research*. Cambridge University Press, 496 pp.

Walton, T. L., and W. D. Adams, 1976: Capacity of inlet outer bars to store sand. *Proc. 15th Coastal Engineering Conf.,* Honolulu, Hawaii, ASCE, 1919–1937.

Winant, C. D., 2007: Three-dimensional tidal flow in an elongated, rotating basin. *J. Phys. Oceanogr.,* **37,** 2345–2362.

——, 2008: Three-dimensional residual tidal circulation in an elongated, rotating basin. *J. Phys. Oceanogr.,* **38,** 1278–1295.

——, 2010: Two-layer tidal circulation in a frictional, rotating basin. *J. Phys. Oceanogr.,* **40,** 1390–1404.